NIPES

Journal of Science and Technology Research

Journal homepage: www.nipesjournals.org.ng

Analysis of the Wear Resistance of Epoxy-Agro Waste Nanoparticle Coating for Mild Steel

Oisakede M. O and Sadjere E. G.
Department of Mechanical Engineering, University of Benin, P.M.B 1154, Benin City, Nigeria
*maureen.oisakede@uniben.edu

Article Info

***Keywords*:**
Mild steel, Epoxy, Nanoparticles, Eggshell ash, Palm kernel ash, Anti-wear properties

Received 07 May 2022
Revised 18 May 2022
Accepted 29 May 2022
Available online 20 June 2022

https://doi.org/10.37933/nipes.e/4.2.2022.29

https://nipesjournals.org.ng

Abstract

Epoxy has been widely used as a coating material to protect the steel. However, one of the disadvantages heaved from the curing reaction of extremely cross linked epoxy matrix is brittleness and micro cracks that alter its performance.The analysis of the wear resistance of epoxy-agro waste nanoparticle coating for mild steel was studied. The agro waste (eggshell and palm kernel shell) was successfully produced as nanoparticles using the sol gel method, Epoxy (LY 556) also called Bisphenol-A-Diglycidyl-Ether and hardener tri-ethylene-tetramine (TETA) with commercial designation HY 951 was also used. There was improvement in the wear resistance after coating with optimum condition obtained at epoxy-5wt% Palm kernel ash nanoparticles, applied load (5 N), sliding speed (1 m/s) and sliding distance (3 km). This study has established that epoxy-5wt% Palm kernel ash nanoparticles have good anti-wear property.

1.0 Introduction

Steels are important construction materials in our modern society. Several processes have been employed in the past to protect metallic substances, polymeric coatings are among the materials that are used to protect metals from corroding. The effectiveness of the coating is typically dependent on the fundamental properties of the sacrificial pigments, barrier effect, organic film, presence of inhibitors and the interface interaction as regards observance Ayman et al [1]. Previously, epoxy coatings were used to protect steels against wear but epoxy coatings are susceptible to damage by surface abrasion and wear. They also show poor resistance to the initiation and propagation of cracks. Such processes introduce localized defects in the coating and impair their appearance and mechanical strength. Min et al [6]. Nanoparticles can reduce voids in coating as well as prevent epoxy disaggregation during curing because they tend to occupy small hole defects formed from local shrinkage during curing of the epoxy resin and act as a bridge interconnecting more molecules. This results in a more homogenous coating, a reduced total free volume as well as an increase in the cross-linked density. Zhang et al [10]. Industries all over the world, Nigeria not being an exception, produce wastes in large amounts from their various manufacturing and production operations. The use of biomaterials in general and agro-waste in particular is a subject of great interest nowadays not only from the technological and scientific points of view, but also socially, and economically, in terms of employment, cost and environmental issues Dagwa et al [3]. Bio-wastes are produced from a large variety of sources and agro-wastes are a class of these wastes.

Agro-wastes are gotten from animal and plant sources. Some of the animal wastes include feathers, shells (egg, snail, periwinkle, and etcetera), horns, hides and skin, hoofs, bones, etcetera. Plant wastes include palm kernel shells, empty fruit bunches, coconut husks, walnut shells e.t.c. These wastes contribute to the problem of environmental pollution and the growing cost of handling the problems of environmental pollution is a world problem being tackled by various organizations around the world.

This research focused on the development of epoxy-nanoparticles coating using palm kernel shells and egg shells as a possible solution to epoxy coating defects.

2. Materials and method

2.1 Materials

Mild Steel (ASTM/SAE 1013) obtained from Warri, Nigeria, the palm kernel shell was obtained from Nigeria Institute for Oil Research near Benin City, Nigeria and the egg shell was obtained from the local tea seller in Benin City Nigeria. The epoxy (LY 556), chemically belonging to the epoxide family was used in the present work. Its common name is Bisphenol-A-Diglycidyl-Ether. Epoxy provides a solvent free room temperature curing system when it is combined with the hardener tri-ethylenetetramine (TETA) which is an aliphatic primary amine with commercial designation (HY 951), Zetamaster 550 nanoparticle size analyzer, PC-2000 Testometric testing machine, CETR UMT-2 tribometer.

2.2 Method

Mild steel with compositions shown in Table 1 commonly used in the construction of Pipeline was used in this work.

Table 1: Chemical composition of the mild steel

S/N	Metal Elements	Percentage (%)
1.	C	0.130
2.	Si	0.153
3.	Mn	0.630
4.	P	0.060
5.	Cu	0.040
6.	Al	0.030
7.	S	0.010
8.	Cr	0.010
9.	Ni	0.020
10.	Mo	0.010
11.	W	0.088
12.	Fe	98.84

The mild steel was grit blasted using alumina grits with of 60 μm size at a pressure of 3 kg/cm^2,. Samples were then cleaned in an ultrasonic cleaning unit. The weights of samples

were recorded (Appendix A) with a precision electronic balance of ± 0.1 mg accuracy. This procedure was adopted from Smith and Yirmani [8].

The sol gel method was used in the production of Palm kernel shell ash nanoparticles and egg shell ash nanoparticles used in this work.

2.2.1. Determination of the Adhesion Strength of the Specimen

A universal testing machine (PC-2000 Testometric testing machine) was utilized for this procedure (Figure 1). The pull-out method which involves two cylindrical samples being used with the surface of one of the cylinders coated with the material being examined and glued with the epoxy resin to the surface of the other cylindrical sample which is not coated. Before the gluing, the uncoated face was grit blasted. Both cylinders were then controlled with steady tensile load. The adhesion strength of the coat was computed by dividing the maximum load applied at the rupture by the cross sectional area of the sample.

Figure 1: PC-2000 Testometric testing machine

2.2.2. Wear Behaviour Testing of Composite Coating

Taguchi's experimental method was applied for wear analysis. The numbers of process parameters as well as their levels values are given in Table 2.

Table 2: The process parameters and their values at different level

Process Parameter description	Process Parameters	Level 1	Level 2	Level 3
A	Sample(uncoated and coated)	Mild steel	Epoxy-4wt% Egg shell ash nanoparticles	Epoxy-5 wt% Palm kernel ash nanoparticles
B	Applied load (N)	5	10	15
C	Speed (m/s)	0.5	1	1.5
D	Sliding Distance (m)	1000	2000	3000

The standards applied for the parameters and levels (minimum, intermediate, and maximum) in this work is in line with parameters applied in analyzing the wear behavior of mild steel by Song et al [9]. The total degree of freedom for four parameters each at three levels is $8[=4\times(3-1)]$. By Taguchi's method, the total degree of freedom of selected orthogonal array (OA) must be greater than or equal to total degree of freedom required for the experiment. So an L_9 OA (a standard three level orthogonal array) having 8 (9-1) degree of freedom was selected for the experiment (Table 3). This orthogonal array has four columns and nine experimental runs. In the analysis, parameter A was allotted column 1 of the L_9 orthogonal array (Table 3), this was also applied to all the parameter allotted to the different columns of the orthogonal array. Given that experimentation for all test states of the selected orthogonal arrays has been done thrice, three responses were documented.

Table 3: The L9 (3^4) Orthogonal Array (OA) (parameters assigned) with response

S/N	Run order	PARAMETERS TRAIL CONDITIONS				RESPONSE (RAW DATA)			SIGNAL TO NOISE RATIO (db)
		A	B	C	D	R_1	R_2	R_3	
1	3	1	1	1	1	X_{11}	X_{12}	X_{13}	SN_1
2	7	1	2	2	2	X_{21}	X_{22}	X_{23}	SN_2
3	5	1	3	3	3	X_{31}	X_{32}	X_{33}	SN_3
4	1	2	1	2	3	X_{41}	X_{42}	X_{43}	SN_4
5	4	2	2	3	1	X_{51}	X_{52}	X_{53}	SN_5
6	6	2	3	1	2	X_{61}	X_{62}	X_{63}	SN_6
7	9	3	1	3	2	X_{71}	X_{72}	X_{73}	SN_7
8	2	3	2	1	3	X_{81}	X_{82}	X_{83}	SN_8
9	8	3	3	2	1	X_{91}	X_{92}	X_{93}	SN_9
Total						Σ	Σ	Σ	

Wear analysis was done using a Tribometer (CETR UMT-2) (Figure 2), which is useful in measuring tribological quantities such as wear volume, frictional force, and friction coefficient between two surfaces in contact.

The signal/noise ratio was calculated for smaller is better, since the lower the wear rate the higher the wear resistance of the materials. Hence, smaller is better method was used to minimize the signal to noise ratio Rosa et al [7].

$$S/N = -10\log_{10}\left(\frac{1}{n}\sum_{i=1}^{n} y^2\right) \quad (1)$$

From Equation 1, y is the measured value of each response and n is the number of runs.

The analysis of variance (ANOVA) was also used to analyze the design parameters that significantly affect the characteristic quality.

Figure 2: CETR UMT-2 Tribometer

3.Results and Discussion

3.1. X-Ray Fluorescence Analysis of the Nanoparticles

The chemical composition of Palm kernel ash nanoparticles and Egg shell ash nanoparticles was determined by X-ray fluorescence to identify the chemical makeup as represented in Table 4.

Table 4: Chemical constituents of the nanoparticles

Compounds	**SiO_2**	**Al_2O_3**	**Fe_2O_3**	**CaO**	**MgO**	**Na_2O**	**K_2O**	**L OI**
Palm kernel ash nanoparticles	81.27	10.67	0.9	2.32	1.3	0.21	0.2	3.01
Egg shell ash nanoparticles	5.89	1.23	0.01	85.56	1.67	0.50	0.13	4.02

The X-ray fluorescence investigation verified that SiO_2, Al_2O_3 were the main constituents of Palm kernel ash nanoparticles, other oxides like. CaO, K_2O, Na_2O were found in traces. It was also seen that CaO has the highest percentage (85.56%) of the constituent of the Egg shell ash nanoparticles because Calcium is the major constituent of egg shell. The Eggshell ash nanoparticles also has a reasonable amount of SiO_2 (5.89%) and MgO (1.67%). The presence of other compounds such as K_2O, Na_2O, Fe_2O_3 contains percentage less than one.

3.2. Nano-Particle Size Analysis

The results of nanoparticle analysis are a shown in Figure 3. It was observed that Palm kernel ash nanoparticles have a higher percentage by weight than the Egg shell ash nanoparticles. In Figure 3, a bimodal curve for particle distribution having distribution range of 0-200 nm for particle size as well as peaks limit about 72.5nm and 95.5nm were obtained for Palm kernel ash nanoparticles and Egg shell ash nanoparticles respectively.

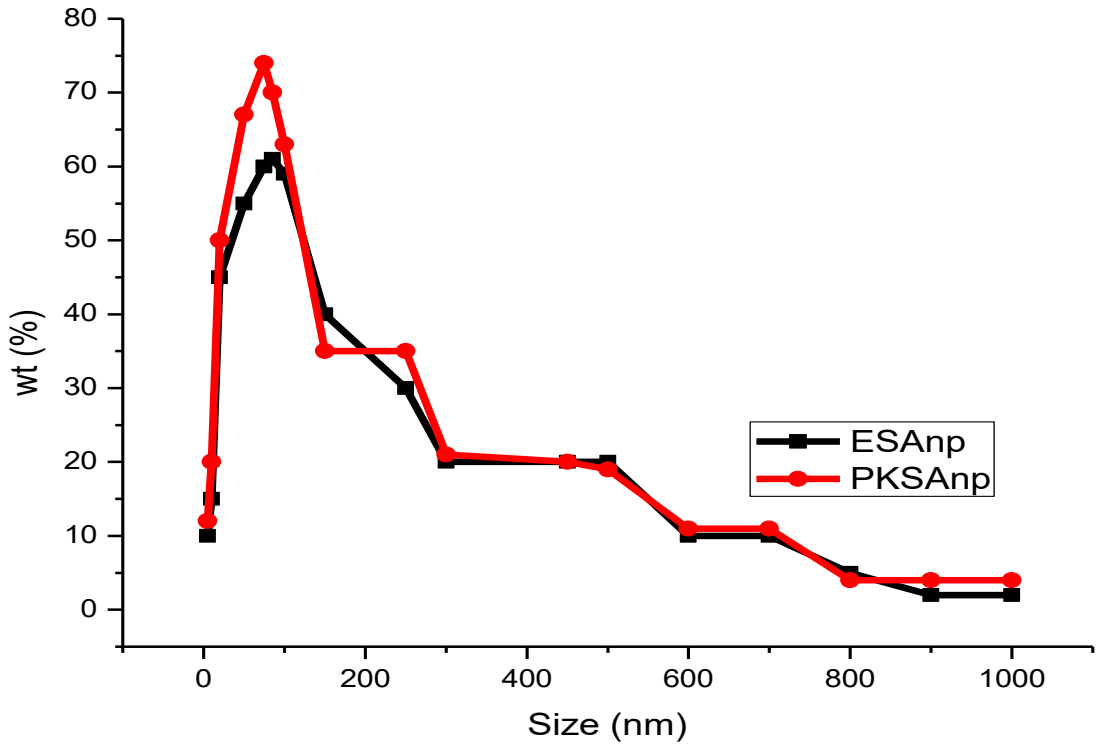

Figure 3: Distribution of particle size in percentage by weight of coating materials

3.3. Adhesion Strength of the coating

Figure 4 and Table 5 show adhesion strength it was seen that graphs of epoxy and that of epoxy composite coatings are similar. Under the stress-strain plot, the composite coatings have a large area. After the maximum strength has been obtained, the brittle nature which generally occurs in epoxy composites, which resulted to the premature failure of the composite coating was not seen.

Figure 4 shows that adhesion strength rises as the percentage weight of Egg shell ash nanoparticles and Palm kernel shell ash nanoparticles increased in the epoxy. Values of 5.32, 7.303, 9.016, 12.32, 15.45, 10.87MPa and 5.32, 7.96, 10.248, 11.559, 12.355, 19.986MPa were obtained for the epoxy-egg shell ash nanoparticles and epoxy- palm kernel shell ash nanoparticles at 0, 1, 2, 3, 4 and 5wt%. Improvement of 190.4 and 275.7% were obtained for epoxy-4wt% Egg shell ash nanoparticles and Epoxy-5wt% Palm kernel shell ash nanoparticles, this can be attributed to the good interfacial bond between the mild steel and coating materials used. This was achieved by the stirring done during the mixing of the composite coating and also the good surface preparation before the coating of the mild steel. The high thermal stress produced at the interface is as a result of the huge change in the coefficient of thermal expansion between the palm kernel shell ash nanoparticles, egg shell ash nanoparticles and epoxy.

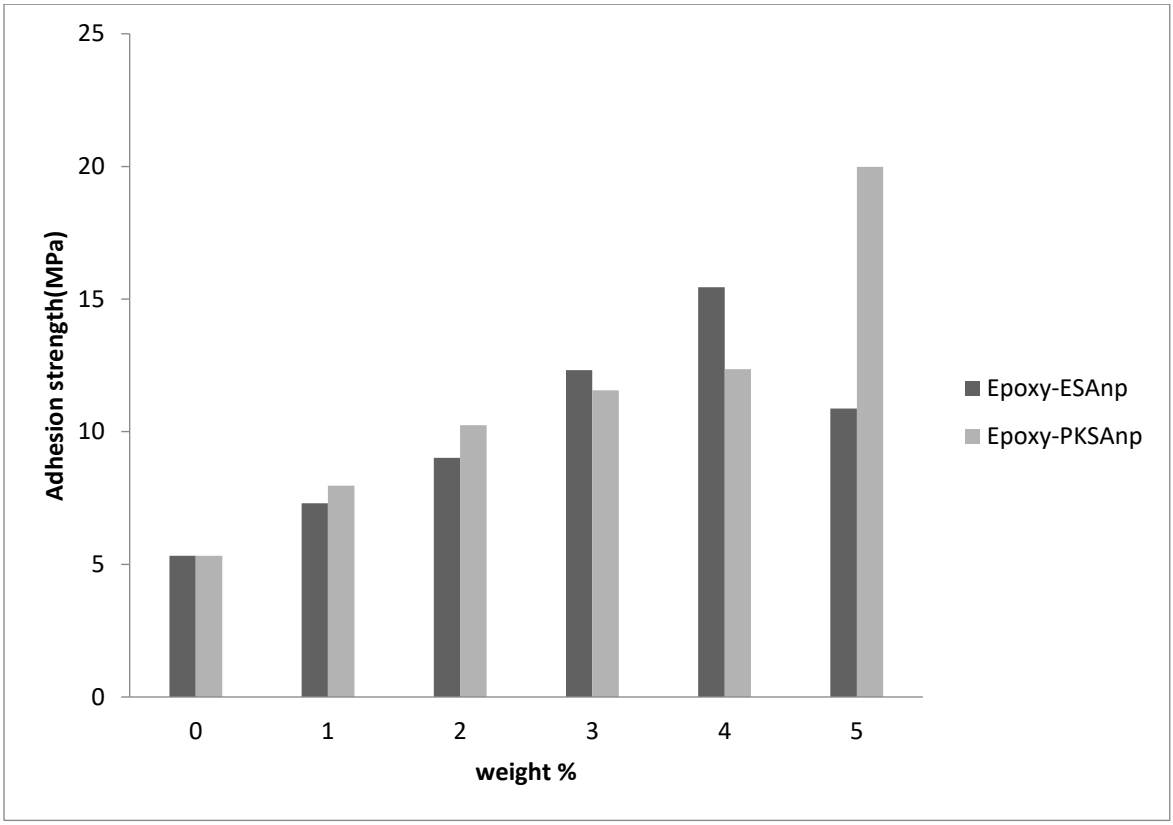

Figure 4: Adhesion strength with percentage by weight coating formulation

Table 5: Adhesion strength with percentage by weight coating formulation

Coating (%)	0	1	2	3	4	5
Epoxy-Egg shell ash nanoparticles	5.32	7.303	9.016	12.32	15.450	10.870
Epoxy- Palm kernel shell ash nanoparticles	5.32	7.960	10.248	11.559	12.355	19.986

3.4. Wear Analysis of the Coating

3.4.1.1. Signals to Noise Effects

Minitab 16.1 software was used for the wear analysis. The outcome of the wear rate is shown in Table 6 while Figures 5 - 9 shows the plots. From Figures 5 - 9, the main effects plot for signal/noise ratio as well as mean to mean of the parameters influencing the wear rate of the composite coatings was shown. In Figure 6, maximum point for each factor showed the paramount level. Observations seen in Figures 5 - 9 shows that as applied load increased, the wear rate also increased, a similar trend was obtained for the sliding speed and sliding distance. With the coating of the mild steel, the wear resistance also improved, this improvement was anticipated because when hardness increases, the flow of stress is restricted thereby, reducing plastic deformation of a material Fayomi et al [5].

Table 6: Different Factor Levels and Parameters for the Experimental Performance

	Sample(uncoated and coated)	Applied load(N)	Sliding speed	Sliding distance(m)	Wear rate(g/m)
S1	1	1	1	1	0.075
S2	1	2	2	2	0.09
S3	1	3	3	3	0.15
S4	2	1	2	3	0.038
S5	2	2	3	1	0.055
S6	2	3	1	2	0.08
S7	3	1	3	2	0.035
S8	3	2	1	3	0.04
S9	3	3	2	1	0.06

From Figures 5 - 9, observation showed that there was increase in wear rate due to an increase in applied load, sliding speed as well as sliding distance, this may be because there is increase in contact time between the material and the disc which in turn increased and thus wear occurred. Also it can be ascribed to elevated pressure at the peak of contact where the quantity of the substrate removed is high. This can be attributed to the separation of particles at more load as well as speed resulting in thermal softening of array material leading to lessening the bonding outcome of the materials.

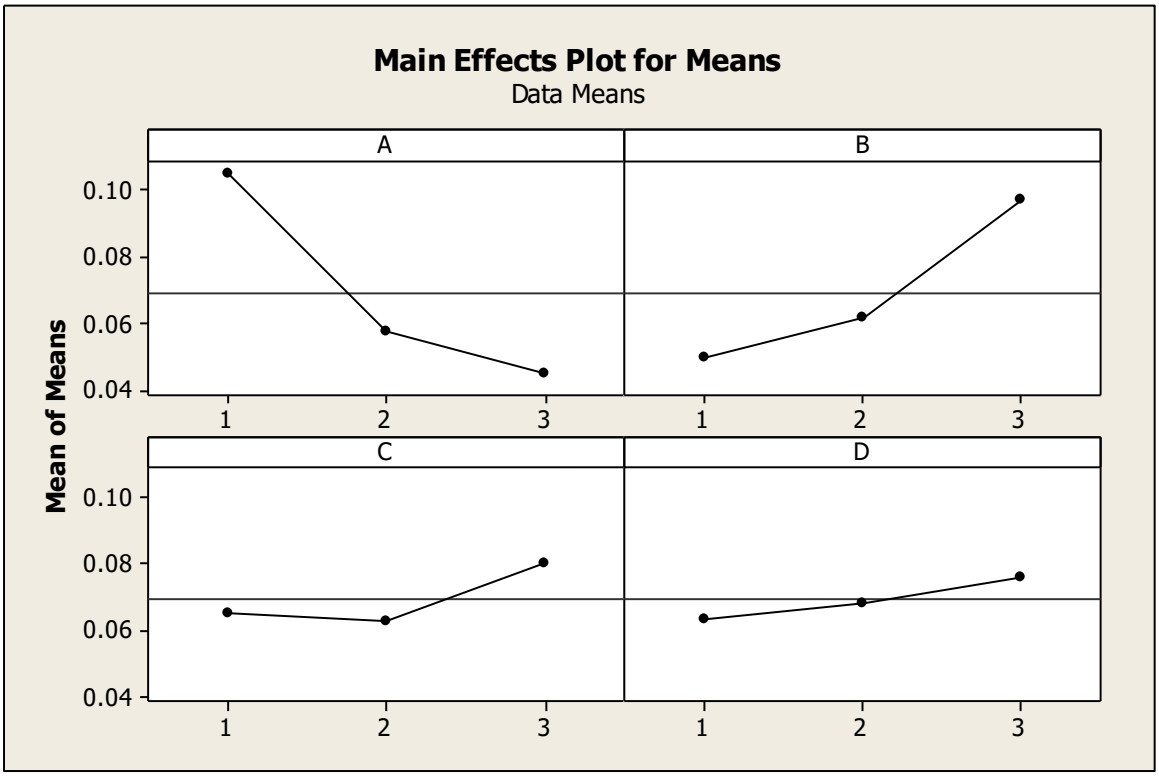

Figure 5: Main effects plot of means

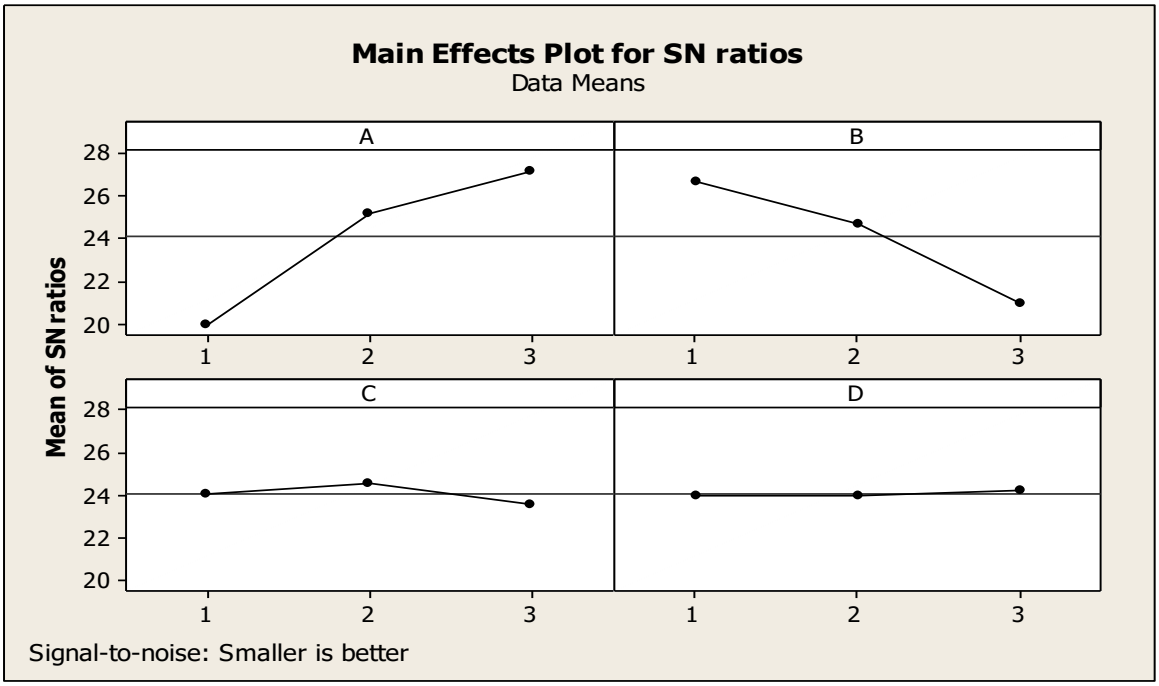

Figure 6: Main effects plot of Signal/Noise ratios

From Figures 5 - 9, it is observed that the coating has positive effect in reducing the wear rate. The wear loss is relatively small when applied load is low, however, the wear rate increased when the sliding speed, applied load as well as sliding distance are increased. Similar observation was seen autonomously for various wear distances as a function of speed and load Eliaz et al [4].

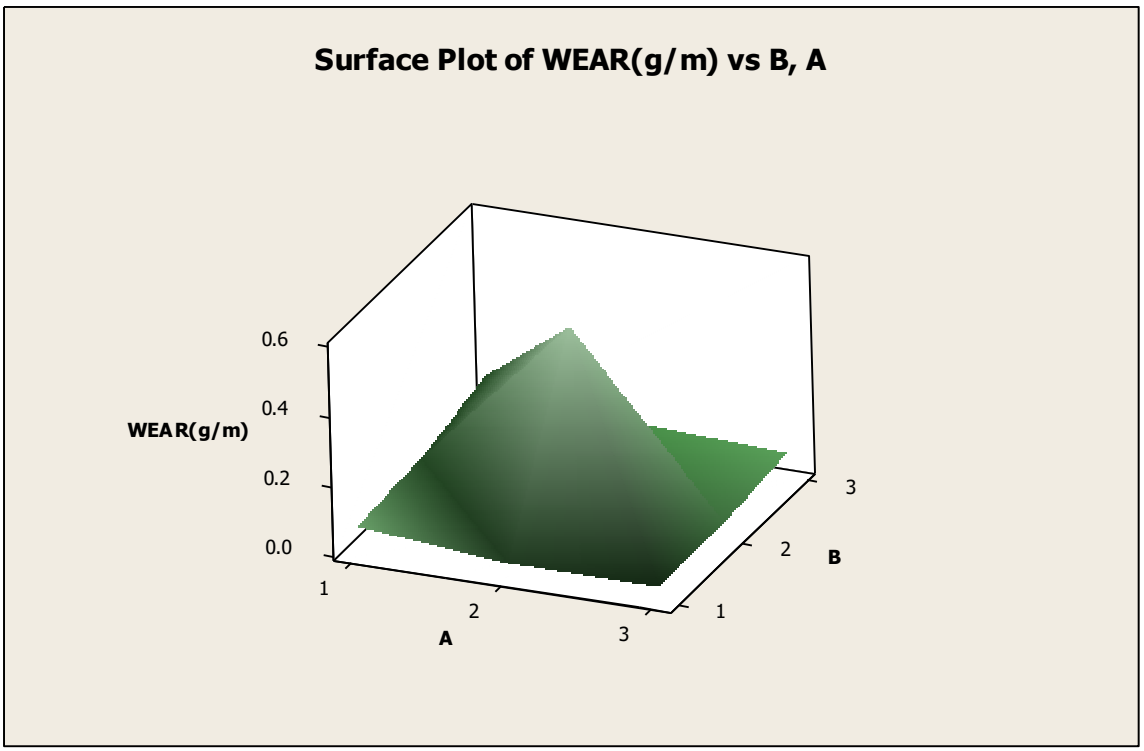

Figure 7: 3 Dimensional plot of coating materials used with applied load

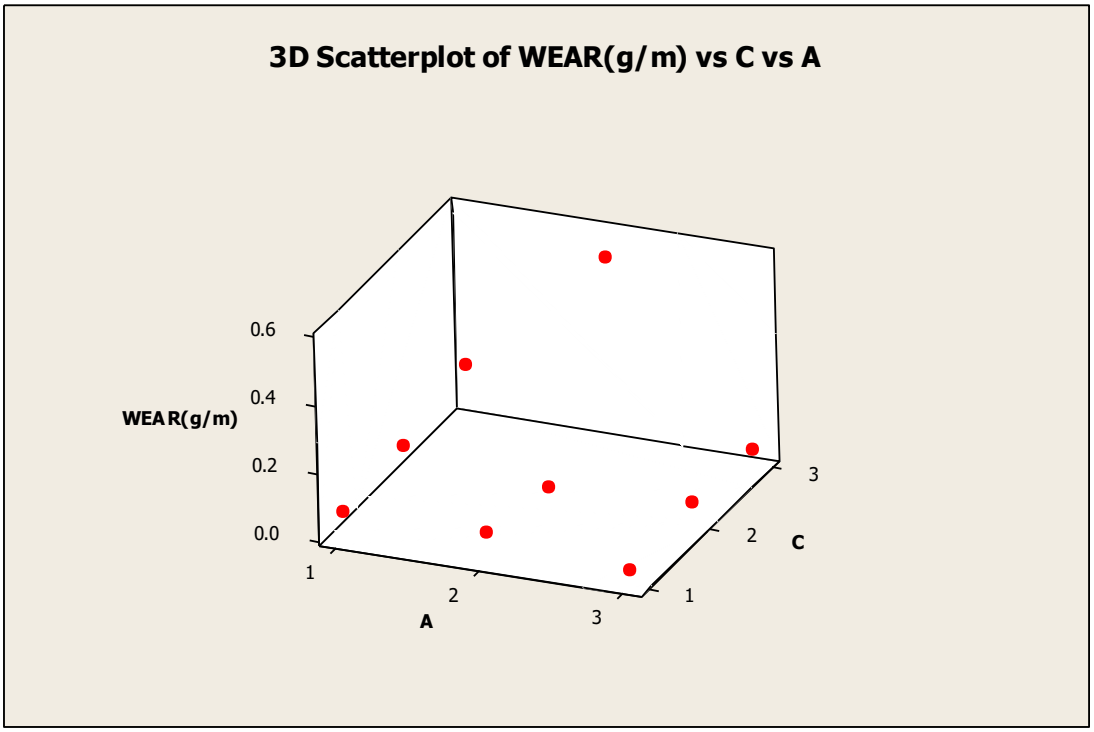

Figure 8: Cube plot of coating materials used with sliding speed

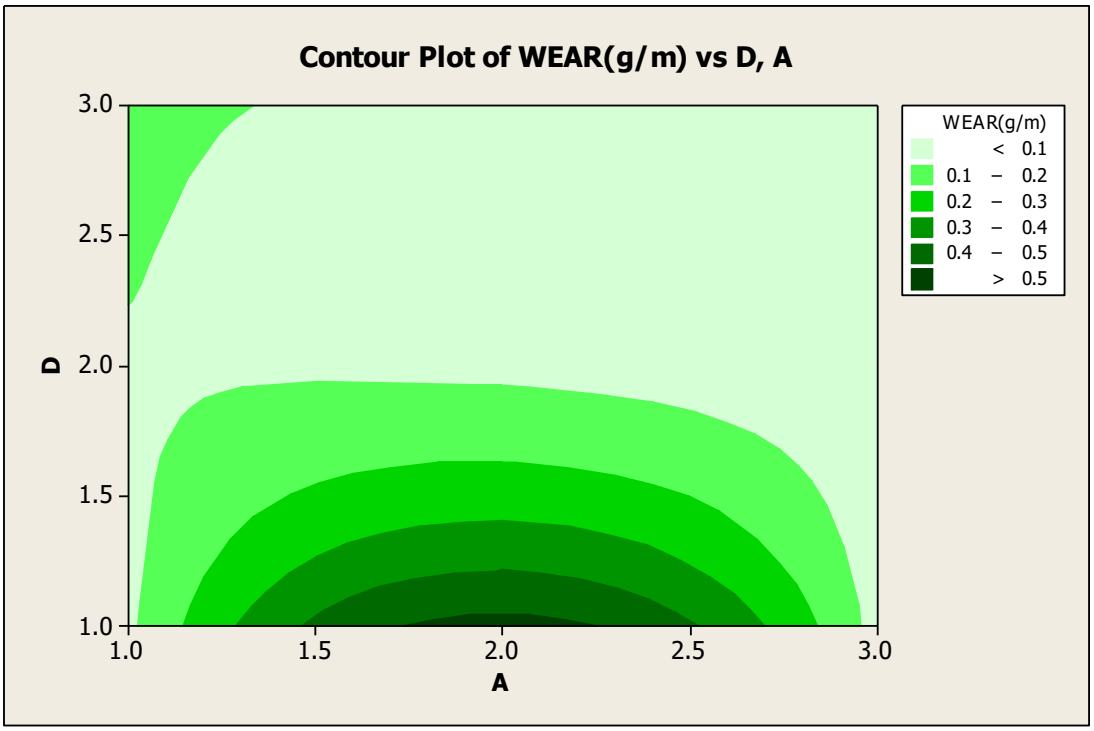

Figure 9: Contour plot of coating materials used with sliding load

3.4.2. Appraisal of the Optimum Performance of the composites coating

Analysis of variance (ANOVA) was performed at a 95% confidence limit to determine the various factors that have the greatest influence on the wear rate.

Table 7: Analysis of variance results of the composites coating

Source	DF	SS	MSS	F	P	%contribution
Model	6	0.17	0.028	1.13	0.5403	
Sample Type	2	0.049	0.025	1.00	0.4993	29.58
Applied load	2	0.051	0.025	1.04	0.4913	30.76
Sliding speed	2	0.066	0.033	1.34	0.4267	39.65
Error	2	0.049	0.024			
Total	8	0.21				

From Table 7, it observed that the sliding speed has the highest contribution of all other factors under investigation, A contribution of 29.58, 30.76, and 39.65% was obtained for the sample type, applied load, and sliding speed respectively. The high effect of the sliding speed was attributed to the forces on the materials and that increased sliding with time. The model can be used to navigate the design since the "Pred R-Squared" of 0.8594 is in reasonable agreement with the "Adj R-Squared" of 0.0871 with a standard deviation of 0.16 and a mean of 0.12.

The Taguchi experimental method was used to analyze the optimum values of wear rate obtained from the experiment. The appraised values of signal/noise ratio and mean for means outcome were obtained using equation 2. Eliaz et al [4].

$$\text{Factors} = \frac{A_1 + A_2 + A_3 + A4}{4} \quad \ldots\ldots\ldots\ldots\ldots\ldots \quad (2)$$

From Tables 8 - 9, it was observed that the parameter levels maximizing the wear rate are Samples used applied load (level 1), sliding speed (level 2) and sliding distance (level 3). Optimum conditions are: epoxy-5wt% Palm kernel ash nanoparticles, Applied load (5N), sliding speed (1m/s) and sliding distance (3000m) (Tables 8 - 9).

Using equation 3, the appraised result of the optimum impact energy was calculated. Eliaz et al [4].

$$WR = AVR + (sample_{opt} - AVR) + (load_{opt} - AVR) + (speed_{opt} - AVR) + (distance_{opt} - AVR) \quad \ldots\ldots\ldots (3)$$

Where, WR= expected response, AVR = average response, $Sample_{opt}$ = mean value of response at optimum setting of factor Sample used, $load_{opt}$ = mean value of response at optimum setting of \factor applied load, $speed_{opt}$ = mean value of response at optimum setting of factor sliding speed, $distance_{opt}$ = mean value of response at optimum setting of factor sliding distance

WR=0.069 +(0.045-0.069) +(0.049-0.069) +(0.063-0.069) +(0.063-0.069)

WR= 0.069-0.024-0.02 -0.006 -0.006

WR=0.013g/m

The investigation was done at the optimum condition where: epoxy-5wt% Palm kernel ash nanoparticles, Applied load (5N), sliding speed (1m/s) and sliding distance (3km) and was used to verify the process parameters. An average value of 0.013g/m was recorded for the wear rate.

Table 8: The Response Table for Means (smaller is better)

Level	Sample	Applied load	Sliding speed	Sliding distance
1 (uncoated sample)	0.10500	0.04933	0.06500	0.06333
2 (coated sample with eggshell)	0.05767	0.06167	0.06267	0.06833
3 (coated sample with Palm kernel shell)	0.04500	0.09667	0.08000	0.07600
Delta	0.06000	0.04733	0.01733	0.01267
Rank	1	2	3	4

Table 9: The Response Table for Signal to Noise Ratios

Level	Sample	Applied load	Sliding speed	Sliding distance
1 (uncoated sample)	19.96	26.67	24.13	24.04
2 (coated sample with eggshell)	25.18	24.69	24.59	23.99
3(coated sample with Palm kernel shell)	27.17	20.95	23.60	24.28
Delta	7.21	5.72	0.99	0.29
Rank	1	2	3	4

Tables 8 - 9 shows that Sample used ranked 1, is the dominant factor, applied load, ranked 2, sliding speed ranked 3 and sliding distance ranked 4 with coating materials having the highest inclination. Interaction plot in Figure 10 gives interaction outcome of control factors on performance characteristic, displaying the minimum result of wear rate at the interaction of samples used, applied load (level 1), sliding speed (level 2) and sliding distance (level 3) (Figure 10).

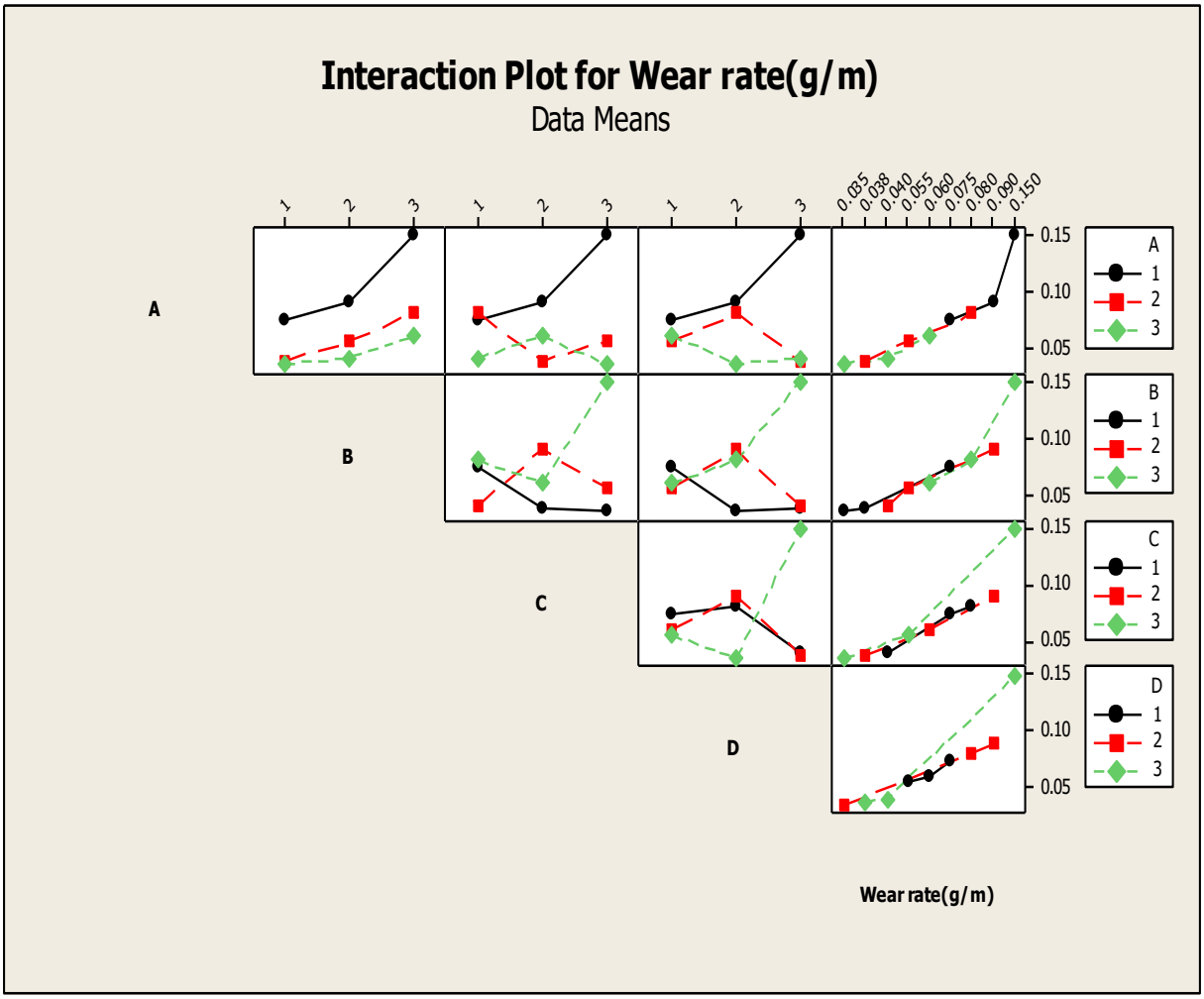

Figure 10: Interaction plot of samples used with all factors

3.4.3. Wear Worn Surfaces

The wear worn surface of the coating is shown in Figures 11 - 13. From the Scanning Electron Microscopy analysis it was observed that there were some differences between the wear surface of the substrate (uncoated sample) and that of the coated sample with that of the substrate showing deep cut, groove and massive plastic deformation of the surface due to wear attack (Figure 11). From Figures 12 - 13 wear scar morphology of the coatings established the permanence of the coatings on the mild steel. When compared with the mild steel, the coated samples showed less damage with less grooving and surface peeling. Similar effect on the reduction of wear damage on the epoxy coated mild steel has been reported by Brostow et al [2].This validates the significant decrease in wear loss achieved from the wear tests that were carried out. Considerable improvement was also observed in the wear resistance accompanied with reduction in wear rate for the coated samples.

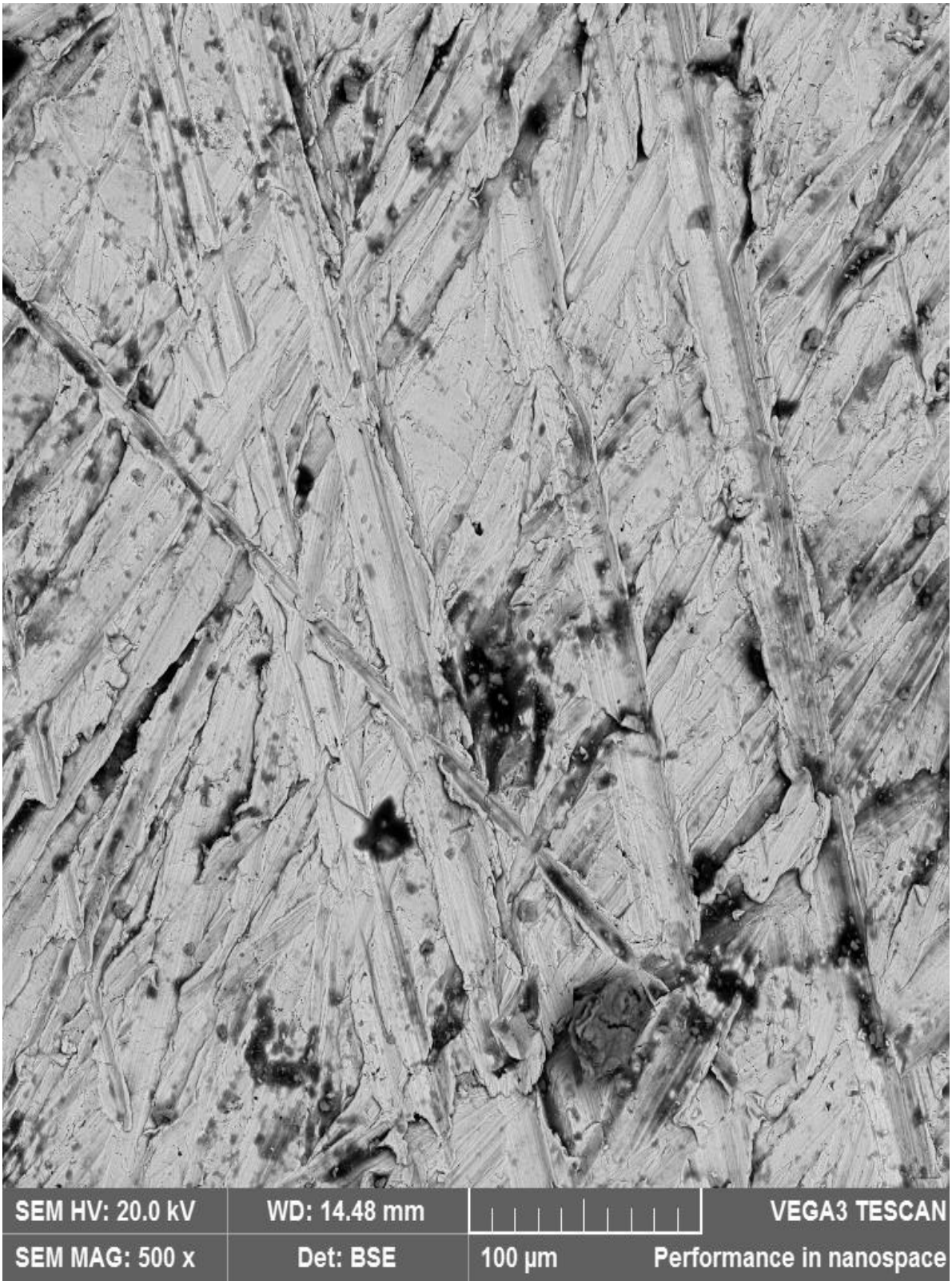

Figure 11: Wear worn surface of the substrate

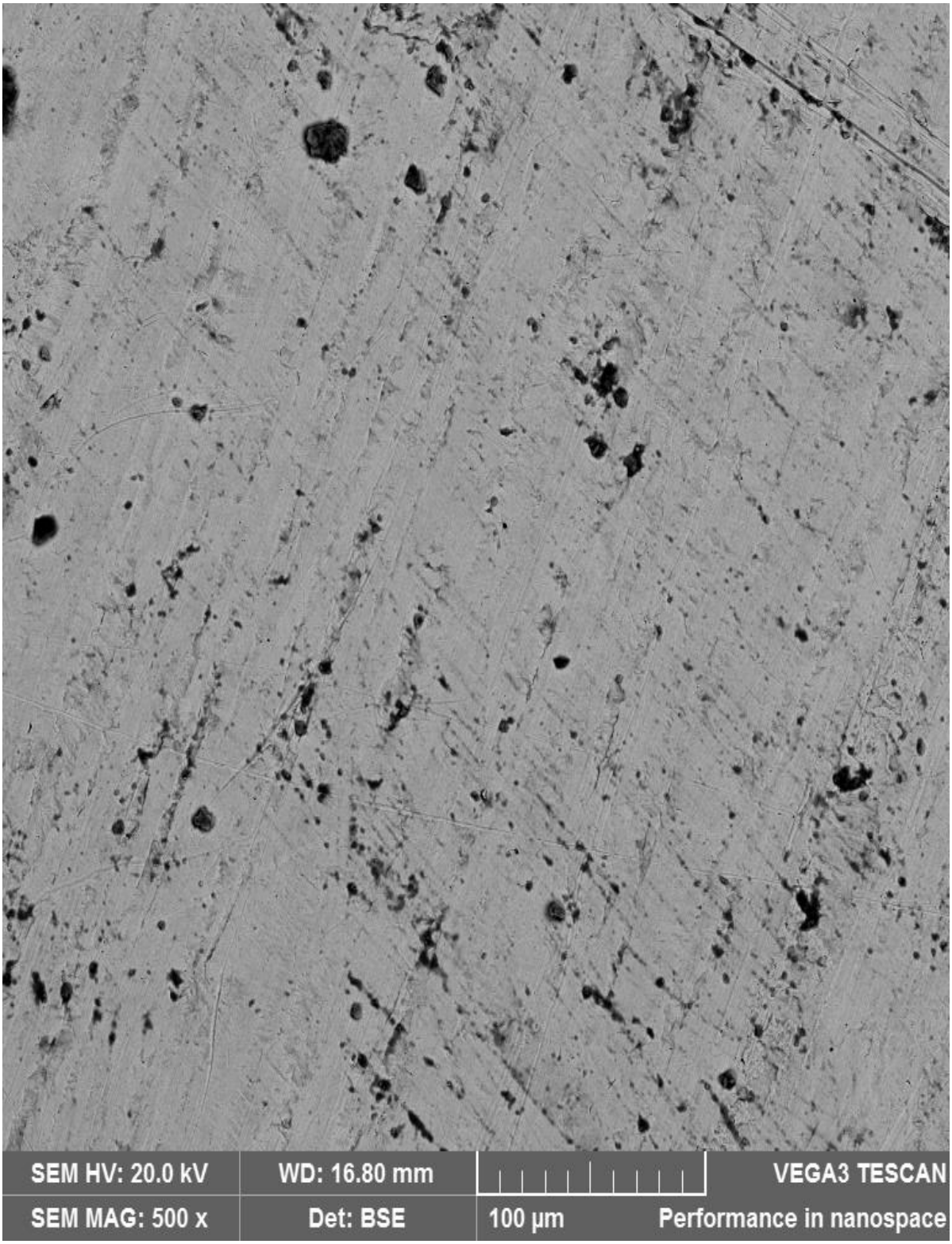

Figure 12: Wear worn surface of the epoxy-4wt% Egg shell ash nanoparticles

Figure 13: Wear worn surface of the epoxy-5wt% Palm kernel ash nanoparticles

4. Conclusion

The development of nanoparticles from agro-waste by-products (eggshell and palm kernel ash) using the sol-gel method was successfully carried out. Characterization of the

nanoparticles as well as the coating of the mild steel was also successfully done and the following conclusions were made:

1. Improvement of adhesion strength of 190.4 and 275.7% were obtained for epoxy-4wt% Egg shell ash nanoparticles and Epoxy-5wt% Palm kernel ash nanoparticles
2. There was improved reduction in wear loss obtained from the wear tests. Significant improvement in wear resistance was observed and drastic reduction in wear rate was seen between the substrate (uncoated samples) and the coated samples,
3. Optimum condition for the wear test was obtained at epoxy-5%wt Palm kernel ash nanoparticles, applied load (5N), sliding speed (1m/s) as well as sliding distance (3km).

This shows that at epoxy-4wt% Egg shell ash nanoparticles and epoxy-5wt% Palm kernel ash nanoparticles we had best properties for anti-corrosion, thermal and anti-wear applications.

Acknowledgement

The first author wishes to specially acknowledge Prof. F. F. O. Orunmwense, Prof. P. O. B. Ebunilo and Dr. E. G. Sadjere for the success of this research work. My thanks also goes to all members of staff of the Mechanical Engineering Department, Faculty of Engineering, University of Benin, Benin City for the success of this work.

Conflict of Interest

There is no conflict of interest associated with this work.

References

[1] Ayman M. A., Hamad A. A., Ashraf M. E., Ahmed M. T. and Mohamed H. W., (2017). Effect of Titanium Dioxide Nanogel Surface Charges and Particle Size on Anti-Corrosion Performances of Epoxy Coatings, *International Journal of Electrochemical Science*, 12 (2), 959 – 974.

[2] Brostow, W., Dutta, M. and Rusek, P. (2010). Modified epoxy coatings on mild steel: Tribology and surface energy. *European Polymer Journal, 46(11), 2181–2189.* doi:10.1016/j.eurpolymj.2010.08.006

[3] Dagwa I. M., and Builders P. F., Achebo J., (2012) Characterization of palm kernel shell powder for use in polymer matrix composites. *International Journal of Mechanical and Mechatronics Engineering.* 12 (4), 88–93.

[4] Eliaz N., Venkatakrishna K. A.and Chitharanjan Hegde, (2010). Electroplating and characterization of Zn–Ni, Zn–Co and Zn–Ni–Co alloys, *Surface and Coatings Technology* 205 (7) 1969–1978.

[5] Fayomi O.S.I., Popoola A.P.I. and Aigbodion V.S. (2015). Investigation on microstructural, anti-corrosion and mechanical properties of doped Zn–Al–SnO_2 metal matrix composite coating on mild steel. *Journal of Alloys and Compounds* 623, 328–334.

[6] Min Z. R., Ming Q. Z., Hong L., Hamin Z., Bernd W. and Klaus F. (2001). Microstructure and tribological behaviour of polymeric nanocomposites. *Journal of Industrial lubrication and tribology.* 53(2), 72-77.

[7] Rosa J. L.; Robin A., Silva M. B., Baldan, Carlos A., Peres and Mauro P., (2009). Electrodeposition of copper on titanium wires: Taguchi experimental design approach". *Journal of Materials Processing Technology. 209 (3),1181–1188.*

[8] Smith J.L. And Yirmani Y.P. (2000). Materials and methods for corrosion control of reinforced and prestressed concrete structures in new construction. *Material sciences*. 165.

[9] Song Q. X., Li G. W., En Z.W., Xiaonan Y. S. (2013). Study on the Wear Resistance of Al_2O_3 Particles Reinforced Epoxy Resin Composite Coating. *Advanced Materials Research*. 821-822, 1148-1151.

[10] Zhang M.Q., M.Z. Rong, S.L. Yu, B. Wetzel and K. Friedrich (2002), Improvement of tribological performance of epoxy by the addition of irradiation grafted nano-inorganic particles, *Macromolecular materials and engineering, 287(2)*, 111-115.